

# Mapping of Epicardial Activation in a Rabbit Model of Chronic Myocardial Infarction: Response to Atrial, Endocardial and Epicardial Pacing

NICOLA L. WALKER, PH.D.,\* FRANCIS L. BURTON, PH.D.,\*† SARAH KETTLEWELL, PH.D.,†  
GODFREY L. SMITH, PH.D.,† and STUART M. COBBE, M.D.\*

From the \*Division of Cardiovascular & Medical Sciences, and †Institute of Biomedical and Life Sciences, University of Glasgow, UK

**Activation Mapping of a Myocardial Infarct.** *Introduction:* This study examines the consequences of a large transmural apical infarct on the epicardial electrical activity in isolated rabbit hearts.

*Methods and Results:* Hearts were isolated 8 weeks after coronary artery ligation. Membrane voltage from the epicardial surface of the left ventricle (LV) including the infarct was monitored using the voltage sensitive dye RH237. Optical action potentials were detected from the epicardial surface of the infarct; the signal amplitude was ~20% of those in the noninfarcted zone (NZ). Epicardial activation mapping of the LV free wall showed that during right atrial (RA) pacing, the activation sequence was not significantly different between infarcted and sham-operated groups. However, direct stimulation of the epicardium in the NZ revealed an area of slow conduction velocity (CV ~5 cm/s<sup>-1</sup>, ~10% of normal values) at the margin of the infarct zone (IZ). Within the IZ, CV was ~50% of normal. A prominent endocardial rim of myocardium in the infarct was not the source of epicardial optical signals because chemical ablation of the endocardium did not affect the epicardial activation pattern.

*Conclusion:* Therefore, remnant groups of myocytes in the mid-wall and epicardium of the infarct scar support normal electrical activation during RA pacing. Areas of delayed conduction emerge only on epicardial stimulation. (*J Cardiovasc Electrophysiol*, Vol. pp. 1-7)

*optical mapping, myocardial infarction, conduction delay, peri-infarct, epicardial pacing*

## Introduction

Myocardial infarction (MI) causes marked changes in the structure and function of both infarcted and surviving myocardium. Six to eight weeks postinfarction,<sup>1</sup> the presence of a connective scar tissue is an important risk factor for ventricular arrhythmias. In the dog model, myocardium bordering the infarct has altered connexin43 expression pattern and fiber geometry.<sup>2-4</sup> These changes generate regions of slow conduction and predispose the heart to re-entrant arrhythmias.<sup>4</sup> Infarct structure varies with species and time after coronary occlusion. In human myocardium, the infarct develops with a less prominent epicardial rim than in canine hearts<sup>5</sup> and a larger surviving subendocardial rim containing several layers of cardiac myocytes in addition to Purkinje fibers.<sup>5</sup> Recent studies examining transmural infarct in the rabbit heart found no significant epicardial rim of myocytes, but a prominent endocardial rim.<sup>6,7</sup>

Epicardial stimulation has been used to reveal conduction abnormalities in experimental MI,<sup>8</sup> but few studies have examined the effects of MI on the activation pattern generated by sinus activity. Furthermore, how pacing site (e.g.,

right atrial, direct endocardial, or epicardial) relates to conduction abnormalities is unclear. This information has a new relevance due to the emergence of bi-ventricular pacing techniques as a method of improving systolic function in patients with LV dysfunction following previous MI.

In this study, a rabbit model (8 weeks post-MI) was used to investigate the consequences of an infarct on epicardial activation during normal ventricular activation (atrial pacing) and direct stimulation of the endocardial or epicardial surfaces of the left ventricle.

## Methods

### Animal Model

A well-characterized model<sup>6,9</sup> of MI induced by coronary artery ligation was studied. Adult male New Zealand white rabbits underwent a left thoracotomy under general anesthesia. The marginal branch of the left circumflex coronary artery was ligated to produce ischemia in 30–40% of the left ventricle (LV). Sham-operated animals underwent thoracotomy with the heart manipulated in identical fashion, except that the artery was not tied. Animals were studied 8 weeks following surgery. The procedure conformed to the *Guide for the Care and Use of Laboratory Animals* published by the US National Institutes of Health (NIH Publication No. 85-23, revised 1996), and the UK Animals (Scientific Procedures) Act 1986.

### Characteristics of the Rabbit Model of LVD

MI animals showed increased LV end-diastolic and left atrial dimension and decreased ejection fraction.<sup>9</sup> Increased

---

This work was funded by the British Heart Foundation.

---

Address for correspondence: Godfrey L. Smith, West Medical Building, University of Glasgow, Glasgow G12 8QQ, United Kingdom. Fax: +44-141-330-4612; E-mail: g.smith@bio.gla.ac.uk

---

Manuscript received 12 November 2006; Revised manuscript received 18 March 2007; Accepted for publication 30 March 2007.

---

doi: 10.1111/j.1540-8167.2007.00858.x

inducibility of arrhythmias and lowered fibrillation threshold were observed *in vitro*.<sup>6</sup>

### Langendorff Perfusion

The hearts were perfused in the Langendorff mode at pH 7.4 and 37°C. Pairs of platinum hook electrodes were placed in the low right atrium. The LV free wall epicardium was stimulated via a pair of bipolar electrodes, which could be moved into different positions on the epicardial surface. The heart was paced at a pacing cycle lengths of 150–300 msec using a 2 msec pulse at twice diastolic threshold. Later experiments used additional bipolar plunge electrodes inserted through the LV free wall to contact the LV endocardial surface. Premature ventricular stimuli (V2) were introduced after every eight regular atrial (A1) stimuli at a cycle length of 250 msec. The A1V2 interval was decreased by 10 msec steps until ventricular refractoriness was observed.

### Optical Mapping

Membrane potential changes were recorded using a photodiode array as previously described.<sup>10</sup> Motion artefact was reduced with three  $\mu\text{mol}\cdot\text{L}^{-1}$  cytochalasin-D (Sigma Aldrich, UK), previously demonstrated to have no significant effect on cardiac activation parameters in rabbits over the range of stimulus frequencies used in this study.<sup>11</sup> The heart was loaded with 100  $\mu\text{L}$  RH237 (Molecular Probes) dissolved in DMSO (1 mg/mL<sup>-1</sup>).

Isochronal maps of activation time were constructed and conduction velocity was derived.<sup>12</sup> The range of activation times in a given heart under specific pacing conditions was defined as the difference in timing between the earliest and latest action potential upstroke recorded by the photodiode array.

### Chemical Ablation of the Endocardium

In some experiments, after initial optical measurements, perfusion was stopped, a 5–6 mm slit was cut in the LV free wall posteriorly, and fluid was drained from the LV cavity. Lugol's solution (0.5–1 mL) was introduced into the LV via a cannula inserted through the slit. The endocardium was exposed to Lugol's for ~5 minutes. In sham trials, perfusing Tyrodes' solution, this procedure did not produce any discernable change in activation pattern (data not shown). Lugol's solution has been previously used to destroy Purkinje fibers and the superficial endocardial cells.<sup>13</sup> In this instance, it was used to ablate the endocardial rim of the LV, including the infarct.

### Histological Preparation

At the end of the electrophysiological study, the hearts were preserved in 5% formaldehyde solution for histology and stereological analysis.

### Statistical Analysis

All data are expressed as mean  $\pm$  standard error. Groups of data were compared with Student's *t*-test (paired when appropriate) or, when there were more than two groups, with one-way ANOVA followed by Tukey-Kramer multiple comparisons.

## Results

### Epicardial Activation Maps Recorded in the Infarct Zone

Photographs of the apical LV epicardium of a sham-operated (sham) and a post-MI heart, with isochronal maps and sample optical action potentials during RA pacing, are illustrated in Figure 1A,B. The infarct zone (IZ) can be identified visually on the basis of the large apical scar (Fig. 1B[i]). Optical action potentials at points along a line extending into the IZ (Fig. 1B[ii] d–f) appeared relatively normal when compared with comparable recordings from the sham heart (Fig. 1A[ii] a–c), but were smaller in amplitude ( $23.2 \pm 3.7\%$ ,  $n = 15$ ,  $P < 0.001$ ) than those in the NZ. These signals were used to examine the time and pattern of epicardial activation. As indicated in Figure 1A(ii), the time for earliest activation was ~20–30 msec later in the MI heart. The minimum time to first epicardial activation was  $86.2 \pm 2.3$  msec in the sham group and  $109.5 \pm 4.0$  msec in MI ( $n = 10$ ,  $P < 0.005$ ). However, the dispersion of epicardial activation, i.e., the time taken for the spread of epicardial activation across the LV including the IZ (Fig. 1B[ii]), was similar to the comparable region of the sham heart (Fig. 1A[ii]). The mean values for the range of recorded epicardial activation times for comparable regions of the LV epicardial surface were  $14.6 \pm 1.1$  msec (sham) versus  $14.3 \pm 0.9$  msec (MI) (NS).

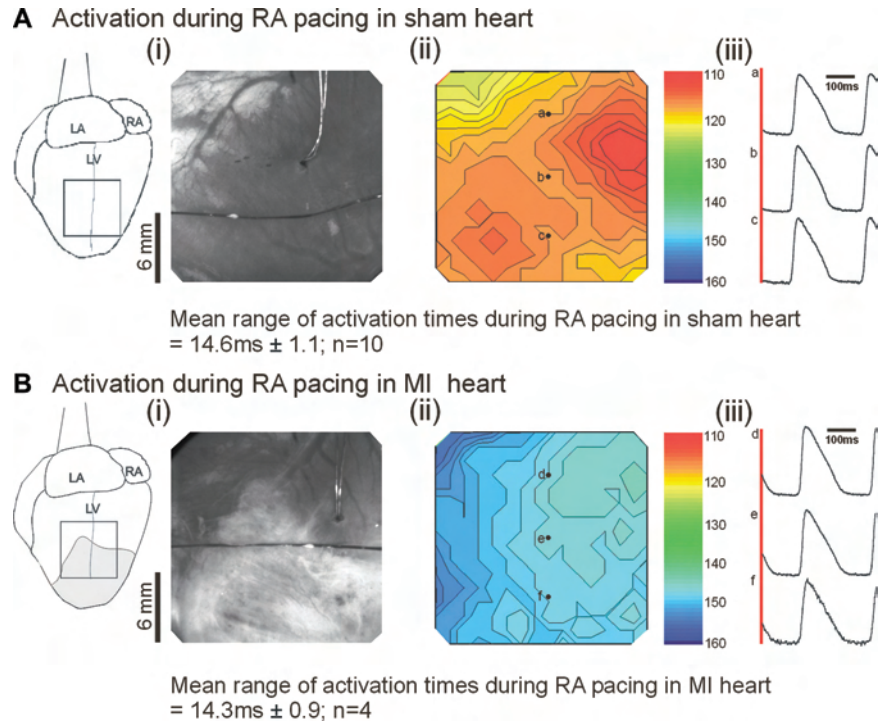
### Stimulation at the Epicardial Surface, but not the Endocardial Surface, Reveals Slowed Conduction in the Peri-Infarct Zone

When the endocardial surface of the noninfarcted LV free wall adjacent to the infarct was stimulated (Fig. 2A[i]), conduction into the IZ showed no evidence of altered epicardial activation pattern (Fig. 2A[ii and iii]). The mean range of epicardial activation times during LV endocardial pacing was  $28.5 \pm 1.7$  msec ( $n = 5$ ). This was not significantly different from the comparable measurement in the sham group ( $29.6 \pm 3.1$  msec,  $n = 6$ , not illustrated). Furthermore, no significant difference in transmural conduction time was observed. The interval from endocardial stimulus to earliest epicardial activation was  $14.7 \pm 3.5$  msec (sham) versus  $14.8 \pm 2.4$  msec (MI) (NS,  $n = 6$ ). Therefore, the presence of the infarct did not appear significantly to affect epicardial activation either during RA pacing (Fig. 1) or pacing on the endocardial surface of the NZ (Fig. 2A).

In contrast, stimulation of the epicardial surface in the NZ adjacent to the scar revealed an area of slowed conduction (Fig. 2B[ii]) at the interface between NZ and IZ (the peri-infarct zone [PZ]). Optical action potentials at points along a line approximately normal to the isochronal lines in the PZ, originating at the point of direct epicardial stimulation and extending into the IZ (Fig. 2B[ii and iii, d–h]), appeared relatively normal apart from (f & g) which had an abnormal upstroke configuration.

Along this line, conduction velocity increased in the IZ once the PZ had been crossed. Slowed conduction in the PZ was a consistent finding in all 10 MI hearts studied (Fig. 3) and was reflected in the larger range of activation times. The mean range of activation times observed in epicardial areas that included an infarct was  $45.5 \pm 3.3$  msec ( $n = 8$ ), compared with  $35.1 \pm 1.4$  msec ( $n = 16$ ) in sham hearts ( $P < 0.01$ ).

**Figure 1.** Epicardial activation during atrial pacing in Sham versus MI A(i) and B(i) show photographs of the epicardial area (18 mm × 18 mm) under study, the horizontal black lines are wires used for epicardial stimulation. The apical infarct scar appears distinctly lighter in the photograph in panel B and is indicated in gray on the schematic diagram. A & B(ii) are isochronal maps of activation. The isochrones (1msec intervals) are relative to the time of stimulation of the RA. Pacing cycle length was 250 msec. Isochrone times (msec) are shown in the adjacent color scale. Sample optical action potentials from the marked positions (a–c & d–f) on the isochronal map are illustrated in A & B(iii); the red vertical line indicates time of stimulus. The mean range of activation times are given below the diagram.



Direct stimulation of the IZ epicardial surface was attempted in all hearts. Pacing in the IZ was successful in 5 out of 10 of the hearts, but required stronger stimuli compared with the NZ ( $3.0 \pm 0.5V$  vs  $0.2 \pm 0.02V$ ). Stimulating in IZ resulted in slowing of conduction at the PZ, with partial restoration of the velocity through the NZ. As shown in Figure 2C(iii)(l–m), optical action potentials recorded from the PZ frequently had biphasic upstrokes suggestive of branched conduction pathways.<sup>14</sup> Furthermore, activation in the IZ displayed anisotropic conduction as in the NZ (Fig. 2C). Accurate determination of the anisotropy axis angle was prevented by the limited size of the infarct. However, along the axis normal to isochrones in the border zone, the mean conduction velocity in the infarct was 29.7 cm/s.<sup>1</sup> Perpendicular to this, the mean velocity within the infarct was 19.4 cm/s.<sup>1</sup> This ratio of longitudinal versus transverse velocities was similar to that observed in the NZ, but conduction velocities in the IZ were ~50% lower than the NZ (Fig. 3). In the five hearts in which epicardial pacing could be achieved in both NZ and IZ, the mean ranges of epicardial activation times were  $45.5 \pm 3.3$  (n = 10) and  $48.0 \pm 2.3$  msec (n = 5), respectively (NS).

Figure 3 summarizes the mean local conduction velocities measured in the NZ, IZ, and PZ along a single axis of activation as indicated in Figure 2B,C. The data were divided according to whether the infarct could be stimulated or not (panels a & b, respectively). Figure 3A shows data separated by epicardial pacing site: NZ(i) or IZ(ii). Conduction in PZ was significantly slower than in either NZ or IZ, regardless of the site of stimulation. Conduction velocities in hearts that could be stimulated in the IZ were not significantly different from those hearts that did not. Optical action potentials recorded from the PZ region may show atypical action potential shape (Fig. 2C, [iii] m–n). These abnormal signals were seen in the PZ irrespective of stimulus origin.

### Effect of a Premature (S2) Stimulus in the NZ on Epicardial Activation

A premature S2 stimulus at an epicardial site was applied during regular RA pacing (Fig. 4). The isochronal maps illustrated are a result of: (a) regular V1 pacing from an epicardial site at the border between the NZ and PZ (Fig. 4[ii]), (b) RA pacing immediately before a premature stimulus (Fig. 4[iii]), and (c) the shortest A1-V2 interval (at a constant stimulus strength) that elicited a response from the epicardial surface (Fig. 4 [iv]). In this case, A1-S2 was 251 msec, which is equivalent to a V2 stimulus 111 msec after the earliest activation of the epicardium. Short epicardial V2 intervals resulted in pronounced slowing of conduction, in contrast to the preceding beat initiated by RA stimulation (Fig. 4 [iii and iv]). The degree of conduction slowing was greater than that seen during regular LV epicardial pacing. Conduction velocity across the PZ was reduced from 8.6 cm/s during regular epicardial pacing to 3.2 cm/s following premature stimulation. However, complete conduction block was not observed. Similar behavior was observed in three other experiments involving extra-stimuli over a range of cycle lengths (150–300 msec). We were unable to induce re-entry by this protocol.

### Histology of Infarct and Surrounding Tissue

A constant feature of all infarcts was a sharp demarcation from NZ to IZ with tongues of scar tissue extending into the NZ (Fig. 5A). On the epicardial side, few surviving cardiomyocytes were present at intermittent points (Fig. 5B[i]). There appeared to be no correlation between the presence of epicardial myocytes with the ability to initiate activation by stimulation on the epicardial surface. A continuous layer of subendocardial surviving cardiomyocytes (200–400 μm thick) was evident in all infarcts (Fig. 5B[ii]). These

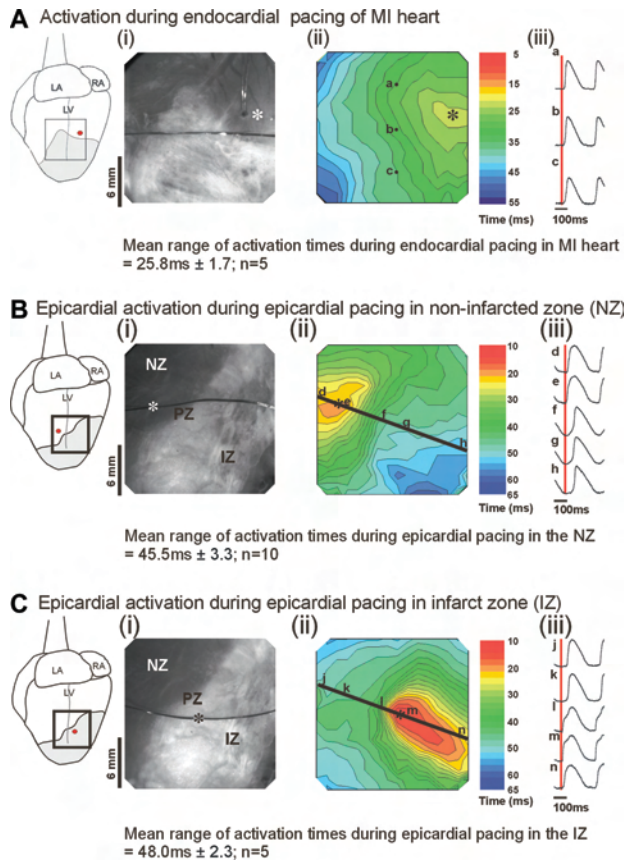


**Figure 2.** Epicardial activation during endocardial or epicardial pacing in MI A, B & C(i) show photographs of the epicardial area under study. Pacing cycle length was 250 msec, stimulation points are shown by asterisks (\*). The isochrones (2 msec intervals) are relative to the time of stimulation of the endocardium (A) or epicardium (B&C). A (ii), isochronal map of activation during endocardial stimulation. B & C (ii), isochronal maps of activation during epicardial stimulation. Isochrone times are shown in the adjacent color scale. Sample optical signals from the marked positions (a–c, d–h & j–n) on the isochronal maps are illustrated in A, B, & C (iii); the red vertical line indicates time of stimulus.

cardiomyocytes appear morphologically normal. Regions of myocytes with pale staining cytosol were observed within the mid-wall of the infarct, some surrounding blood vessels. Average morphological data from six infarcts are shown in Figure 5D. The average wall thickness was  $3.46 \pm 0.22$  mm (n = 6). The average area of each quadrant of the infarct wall occupied by myocytes (identified by cytoplasmic staining) decreased progressively from endocardium to epicardium. The gray box indicates the region occupied by endocardial rim, i.e., a continuous layer of myocardium occupying  $11 \pm 0.5\%$  of the wall. Mean thickness of the endocardial and epicardial rims are  $0.39 \pm 0.04$  mm and  $0.017 \pm 0.012$  mm, respectively.

### Chemical Ablation of the Endocardium

The endocardial rim of myocardium shown in Figure 5 would allow rapid endocardial conduction. Therefore, the regular isochrones observed optically at the epicardial surface may result from either: (1) conduction through the infarct scar to epicardial and mid-myocardial layers, or (2) imaging of purely endocardial activation through the translucent infarct. In an attempt to distinguish between options (1) and

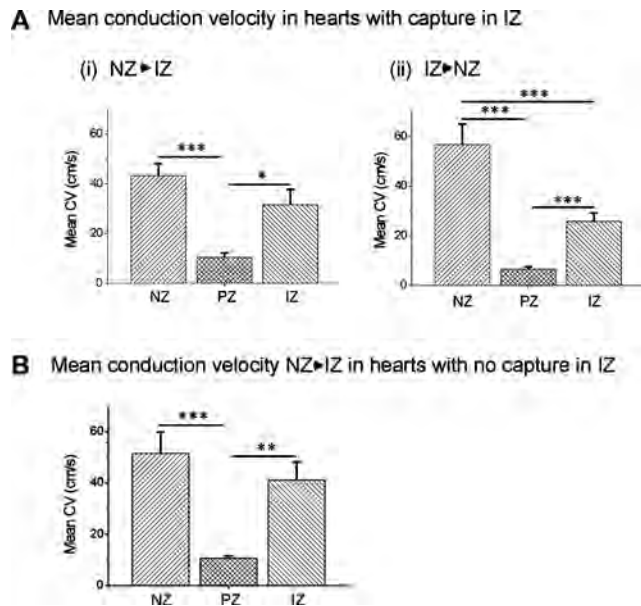


**Figure 3.** Epicardial conduction velocity and potential characteristics. Mean values ( $\pm$ SEM) of conduction velocity measured on an axis normal to the interface between normal zone (NZ) and infarct zone (IZ). The minimum velocity between NZ and IZ was plotted as PZ. A, mean values from MI hearts (n = 5) that responded to direct stimulation in the NZ and IZ. B, mean values from MI hearts (n = 5) that responded to direct stimulation in the NZ but not in the IZ.

(2), the endocardium was treated with Lugol's solution to destroy the immediate endocardial layers. Initial measurements on the intact heart (Fig. 6A[ii]) illustrated normal conduction into the infarct during both RA pacing and endocardial stimulation, as shown previously in Figures 1 and 2. After application of Lugol's solution and re-establishing flow, the resultant optical measurements (Fig. 6A[iv]) show an altered and significantly slower activation pattern on RA pacing. Prior to ablation, the epicardial activation time was  $\sim 25$  msec. After Lugol's treatment, the epicardial activation time increased to  $\sim 60$  msec (Fig. 6). This would imply damage to the endocardium, yet the activation pattern resulting from epicardial stimulation is very similar in pre- and post-Lugol's (Fig. 6B [ii and iv]). This result was observed in three different preparations, suggests that option (2) is the correct pathway, and indicates that significant electrical signal originates within the epicardium and mid-myocardium of the infarct.

### Discussion

It is common to observe groups of myocytes surviving in the subendocardial and subepicardial layers of healed infarcts, the relative sizes of which vary with species. Canine hearts have a well-developed collateral circulation that maintains perfusion of the epicardium after ligation of the left anterior descending or circumflex arteries.<sup>8,15</sup> The subendocardium of healed canine infarcts contains only bundles of Purkinje cells.<sup>16</sup> In human myocardium, the epicardial rim is less prominent<sup>5</sup> and the surviving subendocardial rim contains several layers of cardiac myocytes in addition to Purkinje fibers.<sup>5</sup> The current study (Fig. 5) and previous work<sup>6,7</sup> indicate that the infarct in the rabbit is similar to humans, containing a prominent subendocardial rim of myocytes, but no clear rim of epicardial myocytes. The sparse occurrence

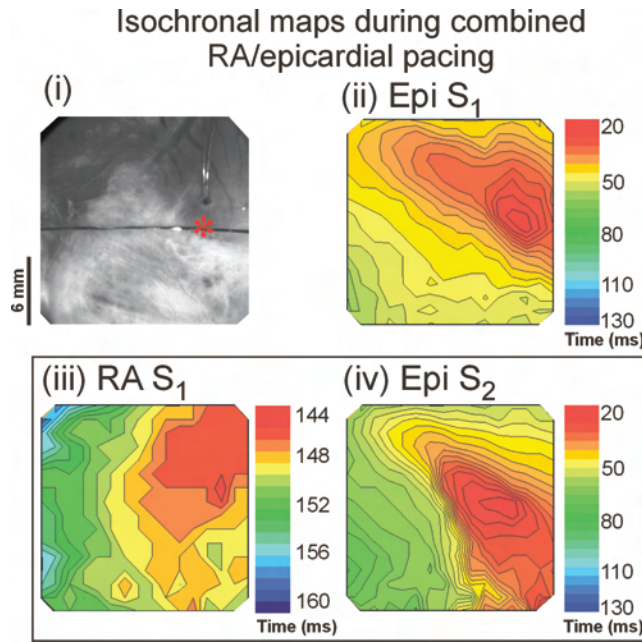


**Figure 4.** Epicardial activation maps after an extra-stimulus. (i) Photograph of the area of epicardial surface under study showing the infarct scar in the lower half of the field. The point on the epicardial surface stimulated by the electrodes is shown by the asterisk (\*). Pacing cycle length (S1) was 250 msec. (ii) Isochronal map (1 msec intervals) of activation during epicardial S1 pacing. (iii) Isochronal map of an epicardial S2 251 msec after pacing of the right atrium.

of myocytes and extensive epicardial fibrosis precluded the use of microelectrodes to study epicardial myocyte electrophysiology.

#### **Epicardial Activation Maps in the NZ of SHAM and MI Hearts**

Although the epicardial activation pattern of the LV free wall in mammals is recognized to be variable, the earliest point of activation most commonly occurs midway between apex and base.<sup>17</sup> In hearts from the MI group, earliest epicardial activation occurred in the mid-ventricular region, but  $\sim 20$  msec later than control. The cause of the extra delay is not known, but preliminary data suggest increased delay at the atrioventricular node.<sup>18</sup>

#### **Epicardial Activation Maps in the IZ**

Despite the presence of a large infarct scar, RA stimulation resulted in well-defined optical signals over the complete area of the IZ (Fig. 1B) similar in time course but smaller in amplitude to those seen in sham hearts (Fig. 1A). Although the optical action potentials are recorded from the epicardial surface, it is unclear to what extent regions deeper within the ventricle wall/infarct contribute to this signal. Histological examination of the infarct indicates the presence of a significant endocardial rim approximately 2–3 mm from the epicardial surface (Fig. 5). Therefore, some of the optical signals could be coming from the myocytes in the endocardial rim. However, there are several reasons to believe that this contribution is not significant. (i) The theoretical depth of focus of the optical system used in this study is 215  $\mu\text{m}$ ,<sup>19</sup> while

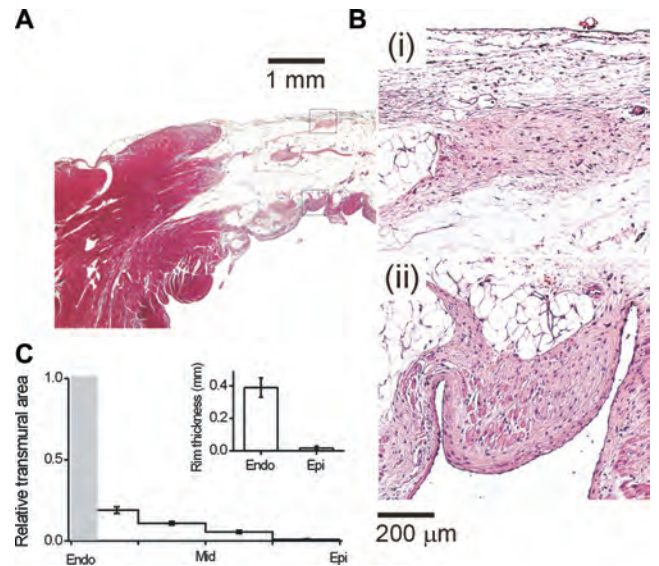


**Figure 5.** Structure of LV wall including infarct A, micrograph of a transverse section of the LV free wall including the infarct stained with hematoxylin & eosin. The rim of epicardial myocytes is shown in detail in B. This rim varies in thickness from sparse to a thicker continuous band below the surface (B(i)). The endocardial rim is thicker ( $\sim 300 \mu\text{m}$ ) and continuous across the entire infarct. Regions of the infarct expanded to panels B(i) & B(ii) are indicated in panel A. Panel C, mean values ( $\pm$  SEM,  $n = 6$  hearts) of relative area of infarct occupied by myocardium. The endocardial rim is indicated in gray.

the infarct wall thickness is  $\sim 3$  mm, (ii) optical transmittance measurements of myocardium and infarct tissue indicate that the fluorescence from the endocardial rim contributes  $< 5\%$  to the total fluorescence detected at the epicardial surface, (iii) different activation patterns are observed in the PZ, depending on whether endocardial or epicardial stimulation is used (Fig. 2); only epicardial stimulation reveals a region of slow conduction at the PZ, and (iv) chemical ablation of the endocardium and His-Purkinje system dramatically affects the activation pattern recorded on the epicardial surface during atrial pacing. This would be anticipated since atrial pacing would normally activate the endocardium first. In contrast, the activation pattern associated with epicardial pacing was unaffected. This supports the assumption that the majority of the signal derives from a predominately epicardial location.

Assuming that the optical signal in the IZ originated from surviving epicardial and mid-myocardial myocytes, it appears that these cells can be activated either via the Purkinje system (RA pacing) or by direct endocardial stimulation, as shown in Figures 1 and 2A and illustrated schematically in Figure 6A. The relatively normal epicardial activation times suggest that the Purkinje system survived intact within the infarct. Furthermore, conduction seems to occur across the wall of the infarct to the epicardium as illustrated in Figure 6A despite the relative absence of myocytes and the presence of connective tissue and fibroblasts in the mid-wall of the scar. Although lacking regenerative currents, fibroblasts can act as passive electrical links between groups of myocytes in culture.<sup>14</sup> Furthermore, fibroblast-myocyte linkage has been observed in rabbit sino-atrial node.<sup>20</sup> This mechanism raises the possibility that the optical signals of change in membrane potential could have originated myocytes and electrically linked fibroblasts.

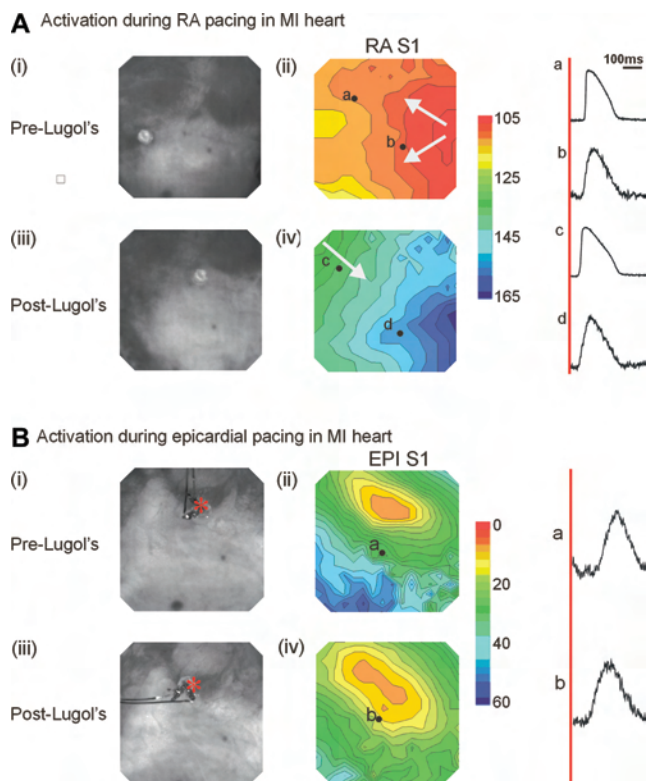


**Figure 6.** Activation patterns after chemical ablation of the endocardium. A & B, (i) & (iii) show photographs of the epicardial area (18 mm  $\times$  18 mm) under study. Pacing cycle length was 250 msec. Panel A, isochronal maps (2 msec intervals) of activation due to RA activation, before (ii) and after (iv) Lugol's treatment. Arrows indicate direction of activation. The isochrones are relative to the time of activation of the RA. B (ii), isochronal maps (2 msec intervals) of activation during epicardial stimulation at the point marked by the asterisks (\*). The isochrones are relative to the time of stimulation of the epicardium. Isochrone times are shown in the adjacent color scale.

Alternatively, transmural conduction may occur via sparse strands of myocytes. While these have been observed spanning healed infarcts in human myocardium,<sup>2</sup> none has previously been shown to link endocardial and epicardial layers functionally.

### Stimulation and Conduction in the Infarct Zone

The isochronal maps indicated that conduction velocities in the IZ were  $\sim$ 50% of control values, yet conduction anisotropy was similar to that observed in noninfarcted tissue. This activity could be due to strands of surviving epicardial myocytes similar to those observed in healed human infarcts.<sup>2</sup> The epicardium of a healed infarct in the canine model of MI shows strands of cells with relatively normal electrophysiology widely separated and disorientated because of ingrowths of fibrous material.<sup>8</sup> This disrupted structure was thought to be the basis of the increased resistances and slowed transverse conduction velocities observed.<sup>8</sup> This scenario is illustrated in Figure 6B(ii). Another possibility is that epicardial stimulation in the IZ resulted in *endocardial* activation as a result of the greater stimulus intensity (3.0 vs 0.2V). However, the delay seen in the PZ during pacing on the epicardial surface of the IZ contrasts with the lack of delay observed during endocardial pacing (compare Fig. 2A,B).

This argues strongly against the direct activation of endocardial myocardium by stimulation of the epicardial surface of the IZ. Conduction pathways within the epicardium or mid-myocardium are more likely to be involved, as illustrated in Figure 6B(ii).

### Slowed Conduction in the Peri-Infarct Zone

Studies have demonstrated redistribution of connexin43 expression around the cell perimeter in myocytes next to an infarct.<sup>2,4,21</sup> These areas correlated with the site of slow conduction and initiation of re-entrant arrhythmias<sup>4</sup> in canine hearts. In the present study, in contrast to the relatively normal activation maps observed in the NZ and IZ during RA pacing or endocardial stimulation, stimulation on the epicardial surface reveals regions of slow propagation at the interface between NZ and IZ (the PZ, Fig. 6B). Conduction velocity fell to approximately 5 cm/s<sup>-1</sup> (10% of normal values) in the 1–2 mm region surrounding the IZ, then increased to  $\sim$ 50% of normal values in the IZ. This slow conduction appears to result from delayed conduction via the epicardial and mid-myocardial PZ rather than the more circuitous route via the endocardium (see Fig. 6B(ii)) since endocardial ablation failed to significantly affect the activation pattern obtained by epicardial stimulation.

### Effects of Endocardial and Epicardial S2 Stimuli during RA Pacing

Application of a close-coupled premature (S2) stimulus generated areas of pronounced slowing (Fig. 4). Thus, although conduction slowing or block are not present during normal (RA) or endocardial pacing, epicardial premature stimulation resulted in areas of pronounced conduction slowing in the PZ.

### Conclusions

This study demonstrates electrical activity on the epicardial surface of large transmural infarcts when ventricular activation occurs via the His-Purkinje system (RA pacing) or via direct stimulation of the endocardium. Remarkably, the infarct scar supports electrical activity that is similar to that observed of normal myocardium. However, stimulation on the epicardium generated areas of slow conduction in the PZ. The conduction velocities observed cannot be accounted for solely by the existence of thin surviving strands of myocytes. We hypothesize that active involvement of electrically in-excitable but coupled fibroblasts is also required.

### References

1. Sun Y, Weber KT: Infarct scar: A dynamic tissue. *Cardiovasc Res* 2000;46:250-256.
2. Smith JH, Green CR, Peters NS, Rothery S, Severs NJ: Altered patterns of gap junction distribution in ischemic myocardium. An immunohistochemical study of human myocardium using laser scanning confocal microscopy. *Am J Physiol* 1991;139:801-821.
3. Peters NS, Green CR, Poole-Wilson PA, Severs NJ: Reduced content of connexin43 gap junctions in ventricular myocardium from hypertrophied and ischemic human hearts. *Circulation* 1993;88:864-875.
4. Peters NS, Coromilas J, Severs NJ, Wit AL: Disturbed connexin43 gap junction distribution correlates with the location of reentrant circuits in the epicardial border zone of healing canine infarcts that cause ventricular tachycardia. *Circulation* 1997;95:988-996.

5. Bolick DR, Hackel DB, Reimer KA, Ideker RE: Quantitative analysis of myocardial infarct structure in patients with ventricular tachycardia. *Circulation* 1986;74:1266-1279.
6. Burton FL, McPhaden AR, Cobbe SM: Ventricular fibrillation threshold and local dispersion of refractoriness in isolated rabbit hearts with left ventricular dysfunction. *Basic Res Cardiol* 2000;95:359-367.
7. Li L, Nikolski V, Wallick DW, Efimov IR, Cheng Y: Mechanisms of enhanced shock-induced arrhythmogenesis in the rabbit heart with healed myocardial infarction. *Am J Physiol Heart Circ Physiol* 2005;289:H1054-H1068.
8. Ursell PC, Gardner PI, Albala A, Fenoglio JJ Jr, Wit AL: Structural and electrophysiological changes in the epicardial border zone of canine myocardial infarcts during infarct healing. *Circ Res* 1985;56:436-451.
9. Ng GA, Cobbe SM, Smith GL: Non-uniform prolongation of intracellular  $Ca^{2+}$  transients recorded from the epicardial surface of isolated hearts from rabbits with heart failure. *Cardiovasc Res* 1998;37:489-502.
10. Choi BR, Burton FL, Salama G: Cytosolic  $Ca^{2+}$  triggers early afterdepolarizations and Torsade de Pointes in rabbit hearts with type 2 long QT syndrome. *J Physiol* 2002;543:615-631.
11. Kettlewell S, Walker NL, Cobbe SM, Burton FL, Smith GL: The electrophysiological and mechanical effects of 2,3-butane-dione monoxime and cytochalasin-D in the Langendorff perfused rabbit heart. *Exp Physiol* 2004;89:163-172.
12. Bayly PV, Kenknight BH, Rogers JM, Hillsley RE, Ideker RE, Smith WM: Estimation of conduction velocity vector fields from epicardial mapping data. *IEEE Trans Biomed Eng* 1998;45:563-571.
13. Chen PS, Moser KM, Dembitsky WP, Auger WR, Daily PO, Calisi CM, Jamieson SW, Feld GK: Epicardial activation and repolarization patterns in patients with right ventricular hypertrophy. *Circulation* 1991;83:104-118.
14. Gaudesius G, Miragoli M, Thomas SP, Rohr S: Coupling of cardiac electrical activity over extended distances by fibroblasts of cardiac origin. *Circ Res* 2003;93:421-428.
15. Wit AL, Allesie MA, Bonke FI, Lammers W, Smeets J, Fenoglio JJ Jr: Electrophysiologic mapping to determine the mechanism of experimental ventricular tachycardia initiated by premature impulses. Experimental approach and initial results demonstrating reentrant excitation. *Am J Cardiol* 1982;49:166-185.
16. Friedman PL, Fenoglio JJ, Wit AL: Time course for reversal of electrophysiological and ultrastructural abnormalities in subendocardial Purkinje fibers surviving extensive myocardial infarction in dogs. *Circ Res* 1975;36:127-144.
17. Durrer D, Dam RTv, Freud GE, Janse MJ, Meijler FL, Arzbacher RC: Total excitation of the isolated human heart. *Circulation* 1970;41:899-912.
18. Walker NL, Burton FL, Cobbe SM, Smith GL: Epicardial activation in isolated rabbit hearts with chronic myocardial infarction. *Biophys J* 2004;86:15a.
19. Girouard SD, Laurita KR, Rosenbaum DS: Unique properties of cardiac action potentials recorded with voltage-sensitive dyes. *J Cardiovasc Electrophysiol* 1996;7:1024-1038.
20. Camelliti P, Green CR, LeGrice I, Kohl P: Fibroblast network in rabbit sinoatrial node. Structural and functional identification of homogeneous and heterogeneous cell coupling. *Circ Res* 2004;94:828-835.
21. Peters NS: Myocardial gap junction organization in ischemia and infarction. *Microsc Res Tech* 1995;31:375-386.